1   **Synchrony and idiosyncrasy in the gut microbiome of wild primates**

2

3   **Authors:** Johannes R. Björk[1*], Mauna R. Dasari[1], Kim Roche[2], Laura Grieneisen[3], Trevor J.
4   Gould[3],   Jean-Christophe Grenier[4,5], Vania Yotova[4], Neil Gottel[6], David Jansen[1], Laurence R.
5   Gesquiere[7], Jacob B. Gordon[7], Niki H. Learn[8], Tim L. Wango[9,10], Raphael S. Mututua[9], J.
6   Kinyua Warutere[9], Long'ida Siodi[9], Sayan Mukherjee[2], Luis B. Barreiro[11], Susan C.
7   Alberts[7,12,13], Jack A. Gilbert[6], Jenny Tung[7,12,13,14], Ran Blekhman[3,15], Elizabeth A. Archie[1*]

8   **Affiliations:**

9   [1] Department of Biological Sciences, University of Notre Dame, Notre Dame, IN 46556, USA

10   [2] Program in Computational Biology and Bioinformatics, Duke University, Durham, NC 27708,
11   USA

12   [3] Department of Genetics, Cell Biology, and Development, University of Minnesota,
13   Minneapolis, MN 55455, USA

14   [4] Department of Genetics, CHU Sainte Justine Research Center, Montréal, QC, H3T1C5,
15   Canada.

16   [5] Research Center, Montreal Heart Institute, Montréal, Quebec H1T 1C8, Canada

17   [6] Department of Pediatrics and the Scripps Institution of Oceanography, University of California,
18   San Diego, San Diego, CA 92093, USA

19   [7] Department of Biology, Duke University, Durham, NC 27708, USA

20   [8] Department of Ecology and Evolutionary Biology, Princeton University, Princeton, NJ 08544,
21   USA

22   [9] Amboseli Baboon Research Project, Amboseli National Park, Kenya

23   [10] The Department of Veterinary Anatomy and Animal Physiology, University of Nairobi, Kenya

24   [11] Department of Medicine, Section of Genetic Medicine, University of Chicago, Chicago, IL
25   60637, USA

26   [12] Department of Evolutionary Anthropology, Duke University, Durham, NC 27708, USA

27   [13] Duke University Population Research Institute, Duke University, Durham, NC 27708, USA

28   [14] Canadian Institute for Advanced Research, Toronto, Ontario M5G 1M1, Canada

29   [15] Department of Ecology, Evolution, and Behavior, University of Minnesota, Minneapolis, MN
30   55455, USA

31   * Correspondence to: bjork.johannes@gmail.com; earchie@nd.edu

32   **Abstract:** Human gut microbial dynamics are highly individualized, making it challenging to

33   link microbiota to health and to design universal microbiome therapies. This individuality is

34   typically attributed to variation in diets, environments, and medications, but it could also emerge

35   from fundamental ecological forces that shape primate microbiota more generally. Here we

36   leverage extensive gut microbiome time series from wild baboons—hosts who experience little

37   interindividual dietary and environmental heterogeneity—to test whether gut microbial dynamics

38   are synchronized across hosts or largely idiosyncratic. Despite their shared lifestyles, we find

39   strong evidence for idiosyncrasy. Over time, samples from the same baboon were much more

40   similar than samples from different baboons, and host-specific factors collectively explained

41   30% of the deviance in microbiome dynamics, compared to just 3% for factors shared across

42   hosts. Hence, individualization may be common to mammalian gut microbiota, and designing

43   universal microbiome interventions may face challenges beyond heterogeneity in human

44   lifestyles.

45

46   **Introduction**

47   Mammalian gut microbiomes are highly complex, dynamic ecosystems. From these

48   dynamics emerge a set of life-sustaining services for hosts, which help them digest food, process

49   toxins, and resist invading pathogens. Despite their importance, our understanding of gut

50   microbial dynamics, especially the collective dynamics of microbial communities from hosts

51   living in the same population, is remarkably poor (*1*). This gap exists in part because we lack

52   time series data that track gut microbiota longitudinally across many hosts in the same

53   population. As a result, we cannot answer key questions. For example, when host populations

54   encounter shifting environments and resources, does each host's microbiota respond similarly—

55   i.e., in synchrony—or idiosyncratically to these changes? Further, are microbial dynamics

56   especially similar when hosts live in the same social unit or have shared traits, such as age, sex or

57   social status?

58   Answering these questions is important because synchronized host microbiomes could

59   help explain shared microbiome-associated traits in host populations, such as patterns of disease

60   susceptibility (*2, 3*). A high degree of microbiome synchrony could also be good news for

61   researchers working to predict microbiome dynamics because it would suggest that similar

62   ecological principles govern microbiome dynamics across hosts (*4*). There is also theoretical

63   justification to expect some degree of synchrony, as host populations and their microbiomes can

64   be considered a 'microbiome metacommunity' (see e.g., *5, 6-8*). Metacommunity theory predicts

65   that synchrony will arise across microbiomes if hosts experience similar environmental

66   conditions and/or high rates of microbial dispersal between each host's microbiome (*9, 10*).

67   　　　However, even in the presence of synchronizing forces like shared environments and

68   high rates of microbial dispersal, there are many reasons why hosts in a microbiome

69   metacommunity could exhibit idiosyncratic (i.e., individualized) microbiome compositions and

70   dynamics. Idiosyncratic dynamics are expected when the same microbes in different hosts

71   respond in different ways to environmental fluctuations, chance events, and/or interactions with

72   other microbes (*11-14*). These forces are likely to be important in the gut microbiome where

73   priority effects, functional redundancy, and horizontal gene flow can cause the same microbial

74   taxon to perform different functions, play different ecological roles, and exhibit different

75   environmental responses in different hosts (*15, 16*). Furthermore, in humans, gut microbiome

76   dynamics are often described as "personalized" (*17, 18*). However, personalized dynamics in

77   humans are nearly always attributed to large interpersonal differences in diet, medications, and

78   lifestyles (*19-22*), and not to fundamentally different microbiome responses to the environment

79   itself (*19*). If personalized dynamics persist in a different primate species, even in the presence of

80   shared environments, this pattern would suggest that: (i) host-specific dynamics are a common

81   feature of primate gut microbial communities (i.e., are not unique to humans and are not solely

82   attributable to large interpersonal differences in human lifestyles); (ii) predicting gut microbial

83   dynamics in individual hosts may prove difficult; and (iii) microbiome interventions to improve

84   human health may face challenges beyond heterogeneity in human lifestyles, and instead may be

85   related to the fundamental ecological principles that govern the gut microbiome.

86

Data and methods

88   　　　Here we test the degree to which gut microbiome compositions and dynamics in a host

89   population are synchronized versus idiosyncratic using extensive time series data from a

90   population of wild baboons in the Amboseli ecosystem in Kenya (*23*). Baboons are terrestrial

91   primates that live in stable social groups, typically with 20 to 130 members. The 600 baboons in

92   our data set lived in 12 social groups over a 14-year span (April 2000 to September 2013; 5

93   original groups and 7 groups that were fission/fusion products from these original groups; **Fig.**

94   **1A**). The baboons were members of the well-studied Amboseli baboon population (*23*), which

95   has been studied by the Amboseli Baboon Research Project since 1971. This project collected

96   detailed longitudinal data on the weather the animals experienced; their social group

97   memberships, ranging patterns and diets; and host traits such as age, sex, social relationships,

98   and dominance ranks (see Supplementary Materials).

99   　　Importantly, like many natural host populations, the Amboseli baboons experience shared

100   diets, environments, and opportunities for between-host microbial dispersal that could drive

101   microbiome synchrony across hosts. Because baboons are not territorial, all 12 baboon social

102   groups used an overlapping ~60 km^2 range (**Fig. 1B**; **video S1**; (*24*)). Hence all animals were

103   exposed to similar microbes from the environment and shared seasonal changes in rainfall and

104   temperature (*24-26*). The Amboseli ecosystem is a semi-arid savanna where very little rain falls

105   from June to October, with highly variable rainfall between November and May (**Fig. 1C**; mean

106   annual rainfall between 2000 and 2013 was 319 mm; range = 140 mm to 559 mm). These

107   seasonal shifts in climate drive a rotating set of foods consumed by the baboons: during the dry

108   season the baboons rely largely on grass corms, shifting to growing grass blades and grass seed

109   heads in the wet season (**Fig. 1D**). Within baboon social groups, diets and environments are

110   especially congruent because group members travel together in a coordinated fashion across the

111   landscape, encountering and consuming resources and feeding on the same seasonally available

112   foods at the same time (*24, 27-31*). Group members also groom each other, combing through

113   each other's fur and placing some items in their mouths, which may contribute to host-to-host

114   microbial transmission (*32*). Finally, at the level of individual hosts, host genetic variation has a

115   consistent, albeit modest, effect on gut microbiome composition in this population (*24*). Other

116   host-specific traits, like age, sex, and social status, also lead some individuals to share aspects of

117   their behavior, immune profiles, and physiology, which could also lead to more congruent

118   microbiome dynamics.

119   　　A key advance in our study is longitudinal sampling of gut microbial composition via

120   16S rRNA gene sequencing from fecal samples collected from hundreds of known baboons

121   throughout their lives (**Fig. 1A**). Such dense, long-term, longitudinal microbiome sampling is

122   difficult to achieve in many animals, including humans. The 17,265 fecal samples in our study

123   were collected from baboons who ranged in age from 7.4 months to 27.7 years, spanning these

124   animals' natural lifespans (**fig. S1A**). Each baboon was sampled a median of 19 times, and 124

125   baboons were sampled at least 50 times (**fig. S1B**). On average, these samples spanned 4.3 years

126   of a baboon's life (range = 4 days to 13.2 years; **fig. S1C**), with a median of 35 days between

127   consecutive samples (**fig. S1D**).

128   A large majority of the microbiome samples we use here were published in Grieneisen et

129   al. (*24*), but we include 1,031 additional samples that were generated at the same time using the

130   same methods (they were not included in Grieneisen et al. (*24*) because we lack pedigree

131   information for these hosts). Briefly, we generated 896,911,162 sequencing reads (mean =

132   51,913.6 reads per sample; range = 1021 - 477,241, **fig. S1E**). We retained microbial amplicon

133   sequence variants (ASVs) with a minimum of 3 reads per sample that were seen in at least 20%

134   of the samples, resulting in 341 microbial taxa at the ASV level (mean = 162 ASVs per sample;

135   range = 19 - 311 ASVs; **fig S1F**). DNA concentration and ASV diversity were not predicted by

136   time since sample collection (**fig. S1G, S1H**). Read counts were centered log-ratio transformed

137   prior to all subsequent analyses (*33, 34*).
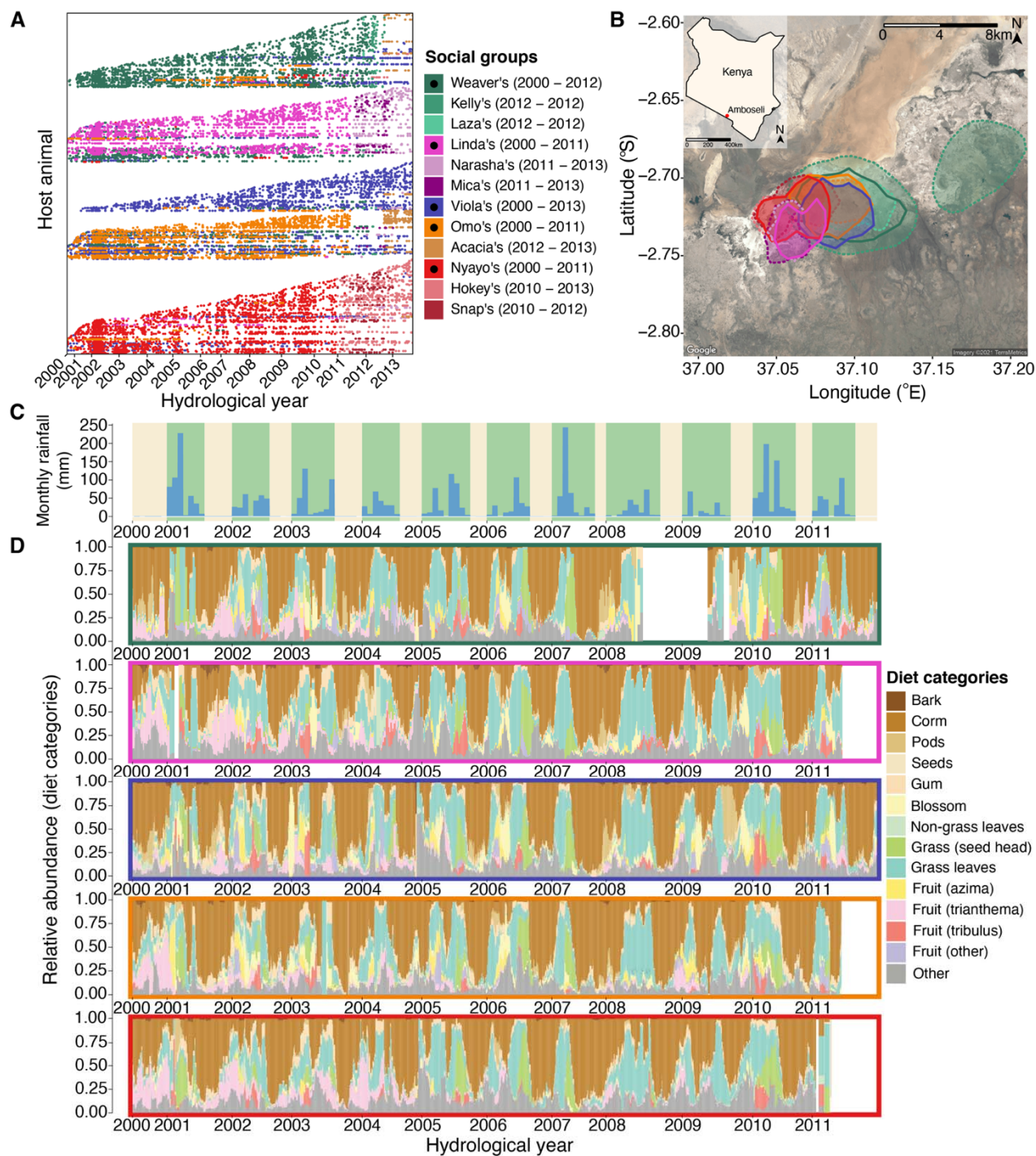
Fig. 1. Baboons in Amboseli experience shared environments at multiple scales. (A) The microbiome time series consisted of 17,265 16S rRNA gut microbiome profiles. Each point represents a microbiome sample, plotted by the date it was collected (x-axis). Each row (y-axis) corresponds to a unique individual host. Samples were collected from 600 wild baboons living in 5 original social groups (indicated by dark colors marked with black dots in the legend) and 7

144   groups that fissioned/fused from these original groups (no black dots). **(B)** All baboon groups

145   ranged over a shared ~60 km^2 area, and the social groups had largely overlapping home ranges.

146   Ranges are shown as 90% kernel densities over the sampling period specific to each group; 5

147   original social groups are shown with solid borders, fission and fusion products with dashed

148   borders. **(C)** Monthly rainfall amounts (blue bars, in mm) with yellow and green stripes

149   representing dry and wet seasons, respectively, with the width reflecting the number of months

150   within the focal year that had at least 1 mm rainfall. **(D)** Temporal shifts in diet from the years

151   2000 – 2013, shown as the relative abundance of diet components in the 5 original social groups

152   over 30-day sliding windows. Colors correspond to the 13 most common food types, while the

153   grey bars correspond to other or unknown food types. Colored boxes around each panel reflect

154   each of the 5 original, most extensively sampled social groups (colors as in plots A and B). The

155   white bars indicate time periods where no diet data were collected.

156

157   To test whether shared environmental conditions and host traits lead to similar gut

158   microbial compositions and synchronized dynamics across the microbiome metacommunity, we

159   used three main approaches (see Supplementary Materials for details of all analyses). First, we

160   characterized patterns of temporal autocorrelation to identify hallmarks of compositional

161   similarity and synchrony over time. Our expectation was that, if different baboons exhibit similar

162   gut microbiome compositions and synchronized microbiome dynamics, then samples collected

163   close in time across the metacommunity should be compositionally similar, and samples

164   collected from the same host should not be substantially more similar than samples from

165   different baboons. Alternatively, if hosts or social groups exhibit idiosyncratic compositions and

166   dynamics, then samples collected close in time from the same baboon, or the same group, should

167   be much more similar than they are to samples collected from different baboons living in

168   different groups. These analyses were run in R (v 4.0.2; (*35*)) using custom-written functions

169   (code and analyzed data are available on GitHub/OSF; see Data Statement).

170   Second, to test whether dispersal limitation could explain microbiome idiosyncrasy, we

171   estimated metacommunity-wide microbial migration probabilities in each season and year using

172   the Sloan Neutral Community Model for Prokaryotes (*36, 37*). This model assumes that each

173   local community, defined as the microbial composition of a single host in a given season-year

174   combination, is the outcome of stochastic population dynamics and microbial immigration from

175   other hosts in the microbiome metacommunity (i.e., other local communities). Briefly, local

176   communities have a constant size N, and individual microbes within each local community die at

177   a constant rate. These deaths create vacancies that can be occupied, either by individuals

178   immigrating from the microbiome metacommunity (with probability m), or by the offspring from

179   any taxon within the local community (i.e., from reproduction within the same host, with

180   probability 1-m). Species that are common in the metacommunity have a higher chance of

181   occupying vacancies than rare species. Without immigration from the microbiome

182   metacommunity, ecological drift leads each host's microbial diversity to reduce to a single taxon.

183   Thus, the migration probability, m, represents the metacommunity-wide probability that any

184   taxon, randomly lost from a given host/local community, will be replaced by dispersal from the

185   microbiome metacommunity, as opposed to reproduction within hosts (36, 37). Following Burns

186   et al. (38), m can be interpreted as a measure of dispersal limitation, such that low migration

187   probabilities signify high dispersal limitation. We estimated season and hydrological year-

188   specific values for m by defining the microbiome metacommunity as either the hosts' social

189   group or the whole host population. We fit neutral models using nonlinear least-squares

190   regression as implemented in the R package tyRa (39).

191   Third, to quantify the relative magnitude of idiosyncratic versus synchronized gut

192   microbiome dynamics for different microbiome features, we used generalized additive models

193   (GAMs) to capture non-linear, longitudinal changes in 52 gut microbiome features, including

194   three principal components of microbial community variation, three indices of alpha diversity

195   (species richness, the exponent of Shannon's H, and the inverse Simpson index, as computed by

196   the function reyni from the R package vegan (40)), and the relative abundances of all 12 phyla

197   and 34 families present in our data set, post filtering. GAMs allowed us to calculate the percent

198   deviance in each feature's dynamics attributable to factors that could contribute to synchronized

199   dynamics at different scales; percent deviance is a measure of goodness-of-fit for nonlinear

200   models and is analogous to the unadjusted R^2 for linear models. We considered three scales:

201   factors experienced by the whole host population (e.g., rainfall and temperature), those

202   differentiated by social groups (e.g., group identity, group home range location, and diet), and

203   those differentiated at the level of individual hosts (e.g., host identity, sex, age, and social

204   dominance rank; see below for complete model structures). If shared environments and traits

8

205   synchronize gut microbiome dynamics across hosts, these factors should explain substantial

206   deviance in microbiome dynamics. Alternatively, if microbiome dynamics are idiosyncratic,

207   population- and group-level factors will not explain considerable deviance and, instead, a large

208   fraction of the deviance will be attributable to host identity, controlling for shared environments,

209   behaviors, and traits. To ensure sufficiently dense sampling for identifying host- and group-level

210   dynamics, all three models were run on a subset of the full data set, consisting of 4,277 16S

211   rRNA gene sequencing profiles from the 56 best-sampled baboons living in the 5 social groups

212   sampled the longest (between 2002 and 2010; min=48; median = 72.5; max = 164 samples; **fig.**

213   **S2**). GAMs were fit using the R package mgcv (*41-43*).

214   Notably, the GAM approach allows us to identify the percent deviance attributable to

215   host identity, but does not identify the specific characteristics that account for host identity

216   effects. Genetic effects are a likely candidate, as previous analyses demonstrate that taxon

217   abundance and summaries of gut microbiome position are lowly to moderately heritable in this

218   population (*24*). To evaluate this possibility, we tested the relationship between the deviance

219   explained in our GAMs for each microbiome taxon and the heritability of that taxon's relative

220   abundance (*24*). If host effects on microbiome dynamics are in part explained by host genotype,

221   we predicted that taxon heritability should be positively correlated with deviance explained at the

222   host level (i.e., model P+G+H), but not at the group or population level (i.e., model P and model

223   P+G).

Results and Discussion

Baboon gut microbiota exhibit cyclical shifts in community composition across seasons and years

We began by visualizing annual and inter-annual fluctuations across the gut microbiome metacommunity over the 14-year span of the data. Consistent with prior research on primates (*44-46*), we found population-wide, cyclical shifts in microbiome composition across seasons and years (**Fig. 2**). This wet-dry seasonal cyclicity was primarily observable in the first principal component (PC1) of a principal component analysis (PCA) of clr-transformed read counts for all 17,265 samples (**Fig. 2A, 2B**; **fig. S3-S5**; PC1 explains 16.5% of the variance in microbiome community composition). PC1 tended to exhibit low values during the dry season, and high values during the wet season, mirroring monthly rainfall (**Fig. 2B; fig. S5**). PC1 was also linked to annual rainfall across years, exhibiting especially low values throughout 2008 and 2009, which corresponded to the worst continuous drought in the Amboseli ecosystem in 50 years (**Fig. 2A, 2B**). We also observed small, but statistically significant seasonal differences in PC2 and PC3 (8.4% and 3.7% of variation in community composition; **Fig. 2C**; **fig. S3-S5**) and in measures of alpha diversity (**Fig. 2C**; **fig. S5, S6**), as has been reported in other ecosystems (*47*).

In terms of individual microbiome taxa, 17% of phyla (2 of 12) and 38% of families (13 of 34) exhibited significant changes in relative abundance between the wet and dry seasons (**Fig. 2C**; **table S1**; linear models with a false discovery rate (FDR) threshold = 0.05 for n = 393 models). These changes were significant for the phyla Firmicutes and Tenericutes (**Fig. 2C, 2D**; **fig. S7**), and were especially pronounced for the families Helicobacteraceae, Coriobacteriaceae, Burkholderaceae, Bacteroidales RF16 group, vadinBE97, Spirochaetaceae, and Campylobacteraceae (**Fig. 2C**; **fig. S8**). 28% of ASVs also exhibited significant changes in abundance across seasons (97 of 341 ASVs; linear models with FDR threshold = 0.05 for n = 393 models; **fig. S9**; **table S2**). The majority of gut microbial taxa at the ASV, family and phylum level did not exhibit significant changes in abundance across seasons, suggesting that these taxa play consistent roles in the gut ecosystem throughout the year, including Kiritimatiellaeota, Elusomicrobia, Ruminococcacaceae, Clostridiaceae 1, and Rikenellaceae (**Fig. 2C**; **fig. S7, S8**; **table S1**).

253
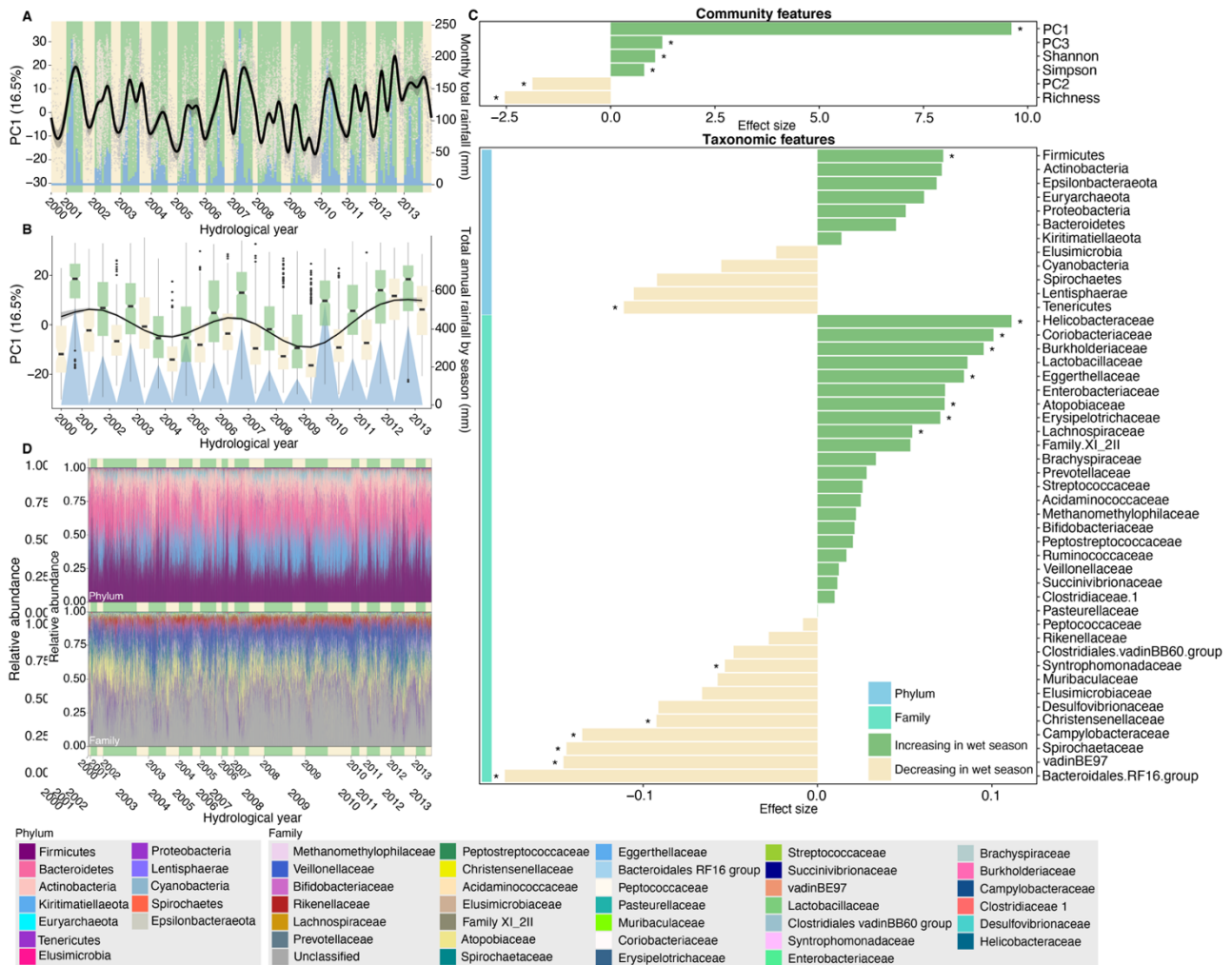
Fig. 2. Baboons show population-wide, cyclical shifts in microbiome composition across seasons and years. (A) Changes in microbiome PC1 mirror monthly rainfall across the 14 years of the data set. The grey points show each sample's value for PC1 (y-axis) on the date it was collected. The black line shows the predicted daily trend for PC1 across samples, treating time (x-axis) as a continuous variable from April 21, 2000 to September 19, 2013. The corresponding gray ribbon shows the 95% simultaneous confidence interval. Blue bars show monthly rainfall (right-hand y-axis). Yellow and green bars in the background represent dry and wet seasons, respectively, with the width reflecting the number of months within the focal year with at least 1 mm rainfall. **(B)** Changes in microbiome PC1 on an annual scale across the 14 years of the data set. The box plots show the average distribution of microbiome PC1 in wet (green) and dry (yellow) seasons. The black line shows the estimated annual trend for PC1 across all hydrological years, and the blue triangles show total annual rainfall (right-hand y-axis). **(C)** The

11

266   effect of season varies across 52 features of the microbiome, including six community features

267   (top panel) and 46 taxonomic features (bottom panel; 12 phyla: light blue vertical bar; 34

268   families: turquoise vertical bar; for 341 ASVs, see Fig. S12). Each horizontal bar shows the

269   effect of season from linear mixed models, with each feature as the dependent variable. Asterisks

270   indicate features that changed significantly between the wet and dry seasons (FDR threshold =

271   0.05 for n = 393 models). See **figs. S7, S8** for feature-specific smooths and **fig. S9** and **table S2**

272   for results for ASVs. Samples from the same host collected on the same date were averaged prior

273   to running the linear models. **(D)** Bar plots showing the relative abundance of all 12 microbial

274   phyla (above) and 34 families (below) across all samples. Green and yellow bars in the

275   background represent wet and dry seasons, with the width corresponding to the number of

276   samples in the focal hydrological year and season.

277

278   **Baboons exhibit largely idiosyncratic gut microbiome compositions and dynamics**

279   While the microbiome metacommunity exhibited cyclical, seasonal shifts in

280   composition, microbiome dynamics across different baboons were not strongly synchronized.

281   Instead, patterns of temporal autocorrelation indicated that each baboon exhibited largely

282   individualized gut microbiome compositions and dynamics (**Fig. 3**). In support, samples

283   collected from the same baboon within a few days were much more similar to each other than

284   they were to samples collected from different baboons over the same time span, regardless of

285   whether those animals lived in the same or a different social group (**Fig 3A, 3B**; Kruskal-Wallis:

286   p < $2.2\text{x}10^{-16}$ for all comparisons). Likewise, a PERMANOVA of Aitchison distances between all

287   samples revealed that host identity explained 8.6% (p < 0.001) of the variation in community

288   composition, much larger than sampling day or month (r^2 = 2.5% and 1.4%), group membership

289   (2.2%), or the first three principal components of diet (0.04% to 2.4%; **table S3**; **fig. S10**).

290   Compositional similarity among samples from the same baboon fell steeply for samples

291   collected a few days to a few months apart (**Fig. 3A, 3C**). However, similarity rose again slightly

292   at 12-month intervals, reflecting the seasonal dynamics in **Fig. 2**. These 12-month peaks in

293   similarity were visible, even for samples collected more than 5 years apart, indicating that

294   individual hosts and the population at large return to somewhat similar microbiome community

295   states on 12-month cycles across years (**Fig. 3C**). Individualized host compositional signatures

12

296   persisted for several years (**Fig. 3A, 3C**; **fig. S11**). Indeed, the 95% confidence intervals on

297   Aitchison similarity between samples collected from the same vs different hosts rarely

298   overlapped for samples collected less than two years apart (**fig. S11B, S11C**).

299   Individualized gut microbiome dynamics can also be seen by visualizing microbiome

300   compositional similarity between hosts living in the population at the same time (**Fig. 3D**; **fig.**

301   **S12**). For instance, especially dense sampling during the 2008-2009 hydrological year meant that

302   we were able to collect at least one sample, for at least 10 months of the year, from 17 of our

303   study subjects. When we aligned these time series, we observed no shared pattern of change in

304   the top three principal components of microbiome composition across time beyond some overall

305   seasonal patterns in PC1, nor did we see convergence to similar values within any given month

306   (**Fig. 3D**). Consequently, the microbiome of each baboon took a different path over the

307   ordination space over the same 1-year span (**fig. S12**). We found similar results for another dense

308   sampling period in the 2007-2008 hydrological year (**fig. S13**).

309   Microbiome taxa varied in their contributions to individualized gut microbiome

310   compositions (**Fig. 3E**; **fig. S14**). For example, for the 56 best-sampled hosts (**fig. S2**), several

311   phyla and families exhibited substantial variation in host mean (clr-transformed) relative

312   abundance (i.e., across repeated samples for that host) compared to their mean (clr-transformed)

313   relative abundance across all hosts. These taxa included members of the phyla Cyanobacteria,

314   Spirochaetes, Lentisphaerae, and Elusimicrobia, and the families Spirochaetaceae, vadinBE97,

315   Elusimicrobaceae, and Muribaculaceae (**Fig. 3E**; **fig. S14**). These highly variable taxa tended to

316   exhibit, on average, below-average abundance compared to less variable taxa that tended to

317   exhibit, on average, above-average abundance, indicating that idiosyncratic dynamics may be

318   more often linked to uncommon than common taxa (**fig. S15**).

319   To test whether individualized gut microbiome compositions and dynamics could be

320   explained by microbial dispersal limitation between hosts, we used the Sloan Neutral

321   Community Model for Prokaryotes to estimate metacommunity-wide migration probabilities, m,

322   for each season and hydrological year (*36, 37*). As described above, m provides a measure of

323   dispersal limitation because it represents the probability that "vacancies" in a local community

324   (i.e. a host's microbiome) will be replaced by the process of dispersal from the microbiome

325   metacommunity (i.e. other hosts), as opposed to reproduction within a focal host's microbial

13

Submitted Manuscript: Confidential

326   community (*36, 37*). We found little evidence that dispersal limitation contributed to

327   idiosyncratic compositions and dynamics; the estimated probability that a given ASV lost from a

328   host's microbiota would be replaced by an ASV from another host in the population was nearly

329   40% (the average host population-wide across season and hydrological years $m = 0.373$; range =

330   0.332 to 0.416; black points on **fig. S16**). These migration probabilities are generally lower than

331   those Sieber et al. (*8*) found for marine sponges sampled from the same coastal location (range of

332   *m* across sponge species: min=0.36; median=0.78; max=0.86) but much higher than for mice and

333   nematodes, both in natural and laboratory populations (mice: $m_{wild} = 0.11$ and $m_{lab} = 0.18$;

334   nematode: $m_{wild} = 0.03$ and $m_{lab} = 0.01$), indicating that dispersal limitation is relatively low for

335   baboon microbiota in Amboseli.

336   Interestingly, when we re-defined the microbiome metacommunity to be the host's social

337   group, instead of the whole host population, migration probabilities were similar (average *m*

338   across groups = 0.355; range = 0.347 to 0.365; colored points on **fig. S16**). Hence, social group

339   membership likely does not represent a large barrier to microbial colonization between baboons,

340   as ASVs are widely shared across all members of the host population.
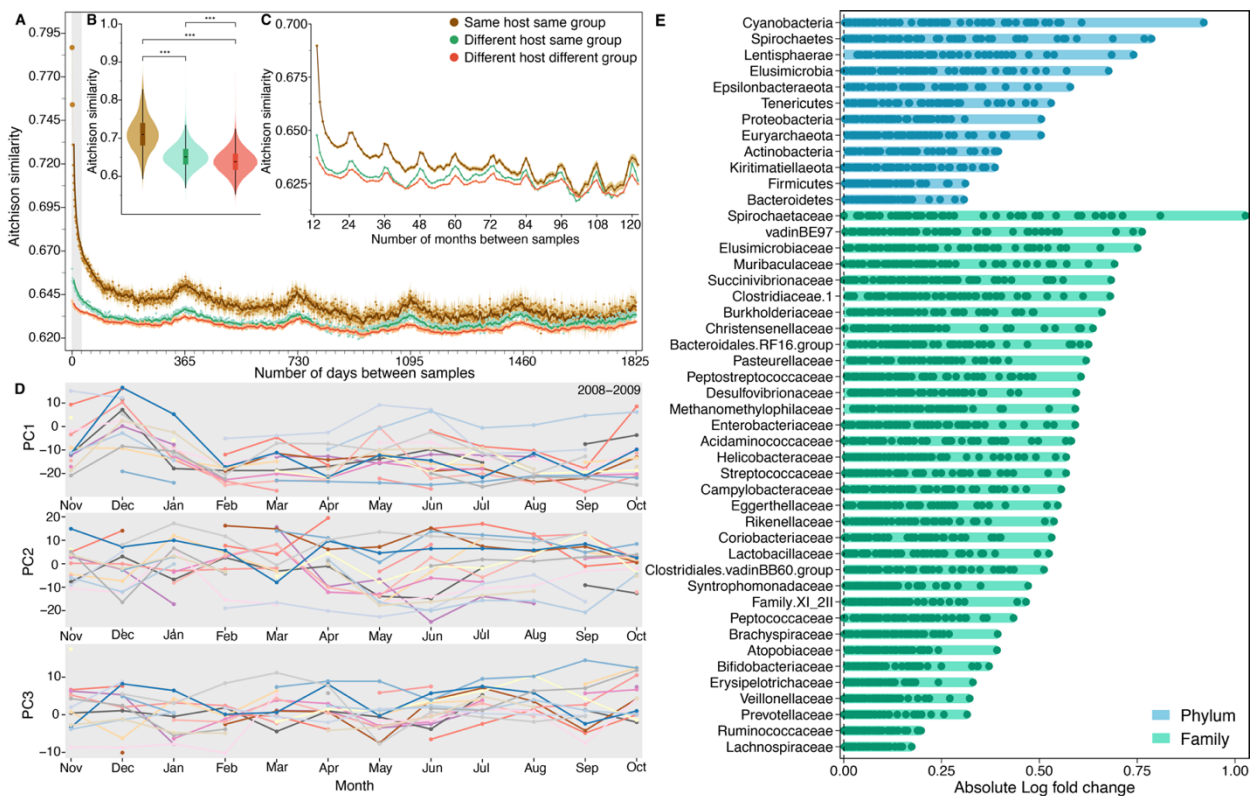

341

342 **Fig. 3. Baboons exhibit idiosyncratic gut microbiome compositions and dynamics. (A)**

343 Temporal autocorrelation in microbiome Aitchison similarity (y-axis) as a function of the time

344 between samples, plotted on a daily scale (x-axis), ranging from samples collected on the same

345 day to samples collected 5 years apart. Small tick marks correspond to months. Brown points

346 show average Aitchison similarity between samples collected from the same baboon; green

347 points show similarity between samples from different baboons living in the same social group;

348 orange points show similarity between samples from different baboons living in different social

349 groups. The lines represent moving averages (window size = 7 days). **(B)** Average Aitchison

350 similarity among samples collected within 10 days of each other. Samples from the same baboon

351 are significantly more similar than samples collected from different baboons in the same or

352 different social groups (Kruskal-Wallis; $p = 2.22 \times 10^{-16}$). **(C)** Temporal autocorrelation in

353 microbiome Aitchison similarity on monthly scales for samples collected up to 10 years apart.

354 **(D)** Microbiome dynamics for 17 baboons for which we had at least one sample from 10 of the

355 12 months of the 2008-2009 hydrological year (Nov 2008 to Oct 2009). Panels show each

356 individual's values for microbiome PC1, PC2, and PC3; each colored line represents a distinct

357 host. See **fig. S13** for similar results during another densely sampled time period. Gaps indicate

358 that the focal host did not have a sample in a given month. **(E)** Some taxa have more

359 idiosyncratic abundances than others. Each horizontal bar shows a given taxon's minimum and

360 maximum absolute log fold change in abundance across the 56 best-sampled hosts (hosts are

361 represented as points within the bars; see **fig. S2** for information on the best-sampled hosts).

362 Absolute fold changes were calculated, for a given taxon in a given host, as the taxon's average

363 clr-transformed abundance across all samples from that host, relative to the taxon's grand mean

364 in all hosts in the population. Hosts with large absolute fold changes for a given taxon therefore

365 have abundances of that taxon that are either well above or below-average compared to its

366 abundance in the host population at large (hosts with points close to zero exhibited taxonomic

367 abundances typical of the population at large). For many taxa, hosts varied in their absolute log

368 ratio values, indicating that they also deviated substantially from each other in the abundance of

369 those taxa. Taxa (y-axis) are ordered (from top to bottom) by their highest absolute log ratio

370 value across the 56 best-sampled hosts. Blue bars represent microbial phyla; green bars represent

371 families. See **fig. S14** for a longitudinal version of this analysis for the most and least

372 idiosyncratic phyla and families.

15

373

Shared environmental conditions are linked to modest synchrony across hosts

To quantify the relative magnitude of idiosyncratic versus synchronized gut microbiome dynamics across the host population, social groups, and individual hosts, and to test whether synchrony varies for different microbiome features, we used generalized additive models (GAMs) to capture the nonlinear, longitudinal changes in 52 microbiome features (3 PCs of community variation, 3 metrics of alpha diversity, and clr-transformed relative abundances of 12 phyla and 34 families). For each feature, we ran three GAMs to measure the deviance explained in gut microbiome dynamics by successive sets of parameters, reflecting the nested nature of our variables (**Fig. 4A**; x-axis of **Fig. 4C**; **table S4**). The population-level model (i.e., model P) captured factors experienced by the whole host population, including average rainfall and maximum daily temperature in the 30 days before sample collection and random effect splines to capture monthly and annual cyclicity in microbiome features (e.g., **Fig. 2A and B**). The group-level model (i.e., model P+G) included all the predictor variables in model P, and added a random effect spline for each social group, as well as variables to capture temporal changes in each group's diet, home range use, and group size (**Fig. 4A, 4C**). The host-level model (i.e., model P+G+H) included all of the predictor variables in model P+G, and added a random effect spline for each host, and variables for host traits, including sex, age, and social dominance rank (**Fig. 4A, 4C**).

Submitted Manuscript: Confidential
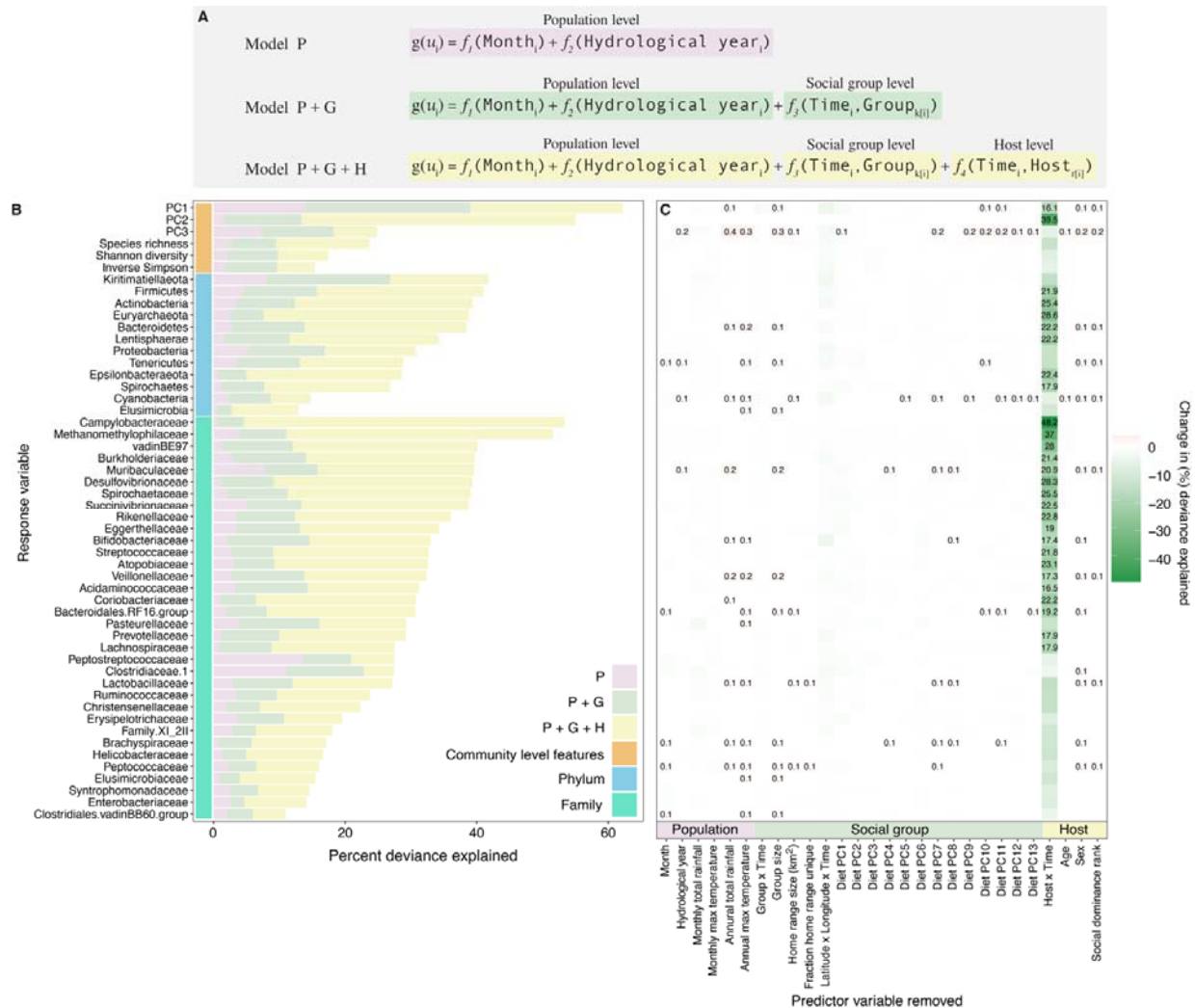
392

393 **Fig. 4. Multilevel modeling identifies idiosyncratic dynamics.** (**A**) We fit three hierarchical

394 GAMs to 52 microbiome features measured in 4,277 samples from the 56 best-sampled baboons

395 living in the 5 social groups sampled the longest (between 2002 and 2010; min=48; median =

396 72.5; max = 164 samples; **fig. S2**). Each model contained successive sets of predictor variables

397 reflecting population-level factors (pink), group-level factors (green) and host-level factors

398 (yellow). The factors at each level are listed at the bottom of panel C and defined in **table S4**).

399 Panel (**B**) shows for each microbiome feature (i.e., response variable), the deviance explained by

400 model P and the successive sets of predictor variables added in model P+G and model P+G+H,

401 respectively (**table S5**). Panel (**C**) shows the loss in deviance explained for model P+G+H as we

402 successively removed each predictor variable in turn from model P+G+H, keeping the model

403 otherwise intact (**table S6**). Losses in deviance are shown in green, and we only provide numeric

Submitted Manuscript: Confidential

404   values for losses in deviance > 15%. Gains in deviance are shown in red; we only show numeric

405   values for gains > 0.1%.

406

407   Consistent with our autocorrelation analyses (**Fig. 3**), comparing the deviance explained

408   for each microbiome feature across the three models revealed primarily idiosyncratic dynamics

409   for most microbiome features (**Fig. 4B, 4C**). Specifically, model P only explained on average

410   3.3% (range = 0.46% to 14.0%) of the deviance across all 52 microbiome features (pink bars in

411   **Fig 4B**; **table S5**), compared to 8.1% on average for adding group-level factors to the

412   population-level model (increase from model P to model P+G; range = 2% to 25%; green bars in

413   **Fig. 4B**; **table S5**), and 30.1% of the deviance for including host-level dynamics (model P+G+H;

414   range = 11.0% to 62.2%) in the same set of features (yellow bars in **Fig. 4B**; **table S5**).

415   Importantly, the added deviance for model P+G+H compared to model P or model P+G was not

416   simply caused by including more parameters. Specifically, randomizing host identity and traits

417   across samples, while keeping each sample's annual, seasonal, and group identity intact, led to a

418   substantial drop in deviance explained relative to the real data (**fig. S17**). For instance, for PC2,

419   which captured the strongest host-level effects of all three PCs, the deviance explained by model

420   P+G+H dropped from 55% to 16.6% when host identity and traits were randomized (**fig. S17;**

421   see supplement and **fig. S18** for an additional analysis investigating the effect of model

422   complexity on deviance explained). That said, for PC3, the addition of randomized host-level

423   dynamics still resulted in more than negligible deviance explained relative to the real data (3% vs

424   6.6%) suggesting that deviance explained may be inflated for some microbiome features.

425   44 of the 52 microbiome features exhibited greater gains in deviance explained by adding

426   host-level factors to model P+G, compared to adding group-level factors to model P, with 22

427   features gaining more than 20% deviance explained between model P+G and model P+G+H

428   (**Fig. 4B**; **table S5**). Three of the most common phyla, Actinobacteria, Bacteroidetes, and

429   Firmicutes all gained >20% deviance explained between model P+G and model P+G+H

430   (Actinobacteria = 27.1%; Bacteroidetes = 24.6%, and Firmicutes = 25.2%; **Fig. 4B**; **table S5**).

431   The most idiosyncratic features (i.e., those that gained >30% deviance explained by adding host-

432   level factors), were microbiome PC2, the phylum Euryarchaeota, and the families

433   Campylobacteraceae, Methanomethylophilaceae and Desulfovibrionaceae (**Fig. 4B**; **table S5**).

434   Notably, even the most synchronous feature, microbiome PC1 (14% deviance explained by the P

435   model), gained 23.2% deviance explained when adding host-level factors to the P+G model.

436   Removing covariates from model P+G+H one at a time, while keeping all other

437   covariates intact, revealed that host identity explained nearly all of the deviance in our models

438   (**Fig. 4C**; **table S5**; average loss in deviance explained by removing host identity = 17.3%

439   compared to 0.2% deviance for all other factors). Beyond host identity, the next most important

440   factor was the geographic area where the group had been travelling in the 30 days prior to

441   sample collection, which on average, explained 1% of the deviance across all 52 features, with

442   the strongest effects on microbiome PC1, Bifidobacteraceae, and Kiritimatiellaeota (**fig. S19**;

443   **table S5**). The removal of all other individual predictor variables had only minor effects on

444   deviance explained (**fig. S19**; **table S5**).

445   To investigate whether some of the idiosyncrasy we observed, especially at the host level,

446   was due to genetic effects, we tested for a relationship between the deviance explained by each

447   GAM and the narrow-sense heritability (h^2) of microbiome taxon abundance as estimated by

448   Grieneisen et al. (*24*). We found that higher levels of deviance explained by model P+G+H were

449   predicted by higher taxon heritability (Pearson correlation: R=0.37, p=0.016; **Fig. 5A**).

450   Reassuringly, we found no such effect at the population or group level, as expected since

451   genotype is a property of individual hosts, not groups or populations (model P+G: R=0.047,

452   p=0.76; model P: R=0.0085, p=0.96; **Fig. 5B**). In particular, we explained substantially more

453   deviance by adding the host level to model P+G for microbiome taxa with moderate to high h^2

454   values (i.e., those > 0.05) than we did for taxa with low h^2 values (model P+G+H: min=16.0,

455   median=32.6, max=53.4 vs model P+G: min=4.6, median=11.1, max=26.8; **Fig. 5B**). These

456   results suggest that some idiosyncrasy in gut microbiome dynamics is a consequence of host

457   differences in genotype. We note, however, that because h^2 estimates from the animal model

458   cannot be mapped directly onto estimates of deviance explained in GAMs, direct estimates of

459   genetic versus environmental effects on host dynamics remain an important topic for future

460   work.

19
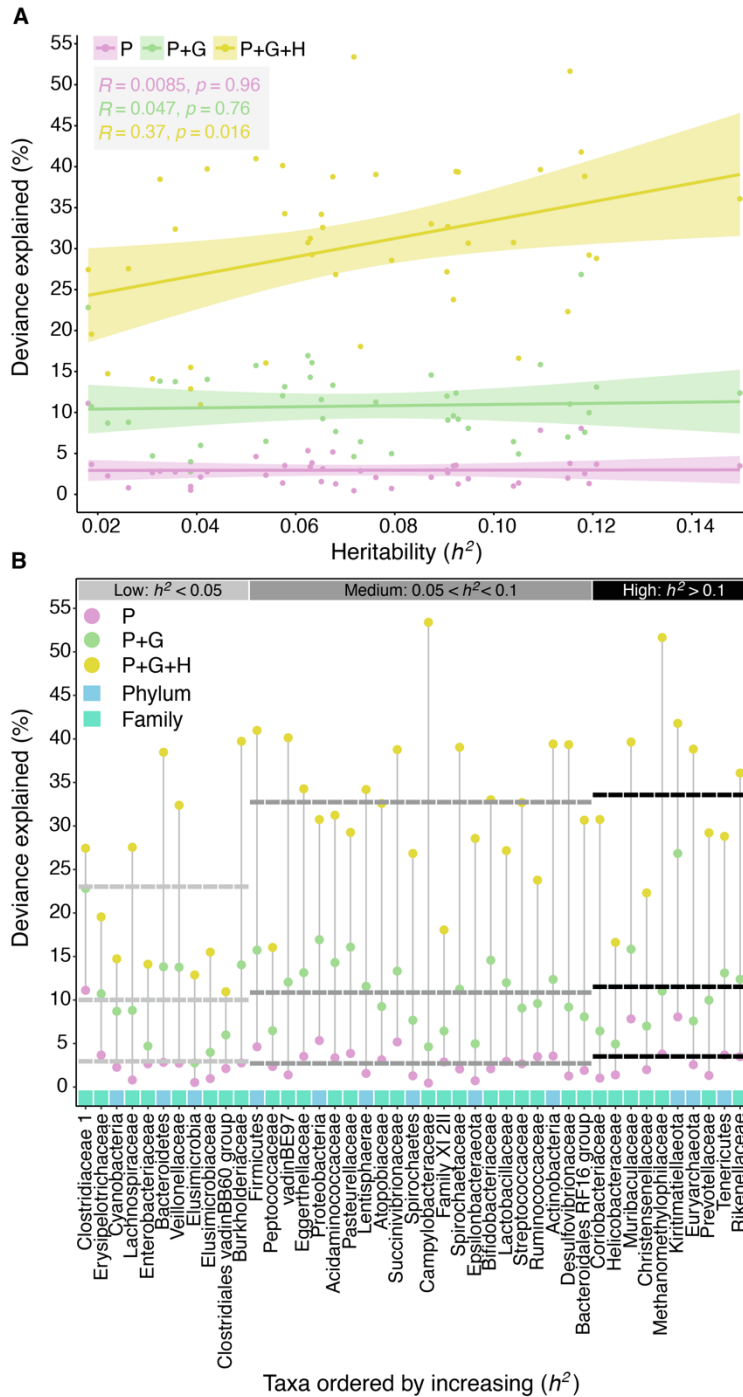
Fig. 5. Microbiome taxon heritability is associated with idiosyncratic dynamics. (**A**) Deviance explained (y-axis) by the phylum and family level GAMs (from **Fig. 4**) plotted against the focal taxon's heritability estimate (h^2; x-axis). Pink, green and yellow denote model P, model P+G and model P+G+H, respectively. (**B**) Deviance explained (y-axis) across the model hierarchy (pink: model P; green: model P+G; yellow: model P+G+H) for each taxonomic feature

Submitted Manuscript: Confidential

467   (i.e., at the phylum and family level; x-axis). The x-axis is ordered by increasing heritability with

468   light blue and turquoise squares representing phyla and families, respectively. Horizontal dashed

469   lines show the average deviance explained per model for taxa with low heritability estimates (h^2

470   < 0.05; light gray); medium heritability estimates ($0.05 < h^2 < 0.1$; dark gray); and high

471   heritability estimates ($h^2 \geq 0.1$; black).

472

473   **Gut microbiome dynamics among social group members are more synchronized than for**

474   **the host population at large**

475   Previous research in humans and other social mammals, including the Amboseli baboons,

476   finds that hosts in the same social group often have more similar gut microbiome compositions

477   than hosts in different social groups (e.g. *32, 48-50*). Likewise, in our current data set, several

478   taxa exhibited abundances that were, on average, higher or lower within a given social group

479   compared to their average abundance in the host population at large (**fig. S20, S21**). Hence, we

480   tested whether shared social group membership is linked to greater microbiome synchrony than

481   hosts in different groups. In support, the patterns of temporal autocorrelation in **Fig. 3A** showed

482   that hosts in the same group have detectably more similar microbiomes than those in different

483   groups, especially for samples collected within 10 days of each other (**Fig. 3B**; Kruskal-Wallis: p

484    $< 2.2\text{x}10^{-16}$). Likewise, samples from the same group tended to occupy similar ordination space

485   over time (**video S2**). While small, these group-level similarities were detectable, even for

486   samples collected more than 2 years apart (**Fig. 3C**; **fig. S11A**). The addition of group-level

487   splines to our GAMs led to gains in deviance that explained more than 10% for 15 of 52

488   microbiome features, including all three microbiome PCs, five phyla, and seven families (**Fig.**

489   **4B, 4C**; **table S5**). Several of these taxa were abundant in hosts, such as Firmicutes,

490   Bacteroidetes, and Bifidobacteriaceae (**Fig. 4B, 4C**; **table S5**).

491   Because each social group has a somewhat distinctive gut microbiota, the effects of

492   climate and diet on microbiome dynamics may differ across groups. To test this idea, we added

493   interaction effects between group identity and climate variables (rain and temperature), or

494   between group identity and the first three PCs of diet to model P+G+H. However, these

495   interactions did not lead to substantial gains in deviance explained in our models (**fig. S22**; **table**

496   **S7**). For instance, adding the climate interactions explained on average an additional 0.95%

497 deviance across all 52 features (range = -1.9% to 5.4%; **table S7**), and diet interactions

498 explained, on average, an additional 1.2% deviance across all 52 features (range = -0.7% to

499 5.6%; **table S7**).

500   Gut microbial congruence among group members could also be linked to shared

501 behaviors and environments: baboons in the same group eat the same foods at the same time,

502 travel as a unit across the landscape, and may be grooming partners that are frequently in

503 physical contact (**Fig. 1B, 1C**; **video S1**; (*24, 27-31*)). Indeed, after host identity, the next most

504 important predictor variable in model P+G+H was the group's home range in the 30 days before

505 sample collection (**fig. S19**; **table S6**). Despite previous evidence for increased similarity in

506 microbiome profiles among grooming partners in the Amboseli baboons (*32*), we did not find

507 evidence for this pattern in our current data set (**fig. S23**). Indeed, samples collected within 30

508 days of each other from individuals with strong grooming bonds were not substantially more

509 similar than samples from animals with weak or no observed grooming relationship (mean

510 Aitchison similarity between pairs with strong bonds = 0.645; mean Aitchison similarity between

511 pairs weak or no bond = 0.646; **fig. S24**). Because of differences in methodology, the lack of a

512 grooming effect in this data set should be interpreted with caution. Our prior research on this

513 topic (*32*) characterized microbial communities using shotgun metagenomic sequencing from

514 >90% of social network members, all within 30 days of each other. In contrast, this current data

515 set relies on 16S rRNA gene sequencing data from sparsely-sampled networks. Shotgun

516 metagenomic data provide much higher taxonomic resolution than 16S rRNA identities, and may

517 therefore more accurately capture the direct transmission between hosts.

518

Conclusions

520   We tested, for the first time, whether gut microbiome dynamics are synchronized among

521 hosts experiencing strong synchronizing forces, including shared environments, similar diets,

522 and high rates of between-host microbial dispersal. Despite these forces, baboons in Amboseli

523 exhibit largely idiosyncratic gut microbiome dynamics: samples from the same baboon collected

524 within a few days of each other were much more similar to each other than samples from

525 different baboons, and host-specific factors, especially host identity, collectively explained 30%

526 of the deviance in microbiome dynamics, compared to just 3% for factors shared across the host

527   population. These idiosyncratic dynamics suggest that microbiome personalization is a

528   widespread phenomenon that is likely not unique to humans, and instead may be shared with

529   other social mammals. This microbiome personalization likely emerges from ecological and

530   evolutionary phenomena that are a normal part of complex microbial communities, such as

531   priority effects, functional redundancy, and horizontal gene flow. Together, these forces are

532   expected to lead microbes with the same taxonomic identity in different hosts to perform

533   somewhat different functions, experience different competitive landscapes and selective regimes,

534   and play different ecological roles (*15, 16*). As a result, the same microbial taxa may often

535   respond in different ways to environmental fluctuations, chance events, and/or interactions with

536   other microbes in different hosts, producing personalized, rather than synchronized dynamics.

537   This personalization means that microbiome research aimed at improving human and

538   animal health could face challenges to developing broadly applicable therapies, beyond those

539   caused by heterogeneity in host diets, behaviors, and environments. Microbiome researchers aim

540   to predict microbiome changes, link microbiome taxa and dynamics to health outcomes, and

541   design microbiome interventions that work well for large segments of the human population.

542   Personalization in humans is already presenting problems in attaining these goals. For instance,

543   predictive models of gut microbiome dynamics from one person have been shown to fail when

544   they are applied to other people (*19*). Our results suggest that microbiome predictions and

545   interventions focused on microbiome taxa will require approaches that are either personalized or

546   focus on microbial functions, as opposed to taxonomic identities. Even then, "universal"

547   microbiome therapies that work the same way for all hosts may be unattainable. Instead,

548   microbiome interventions will likely work best when they are designed for specific host groups

549   or populations that have shared compositions and dynamics. Further, we expect that the types of

550   prediction and intervention efforts that will suffer least from gut microbiome personalization are

551   those that focus on microbiome functional traits (e.g., metabolites; functional pathways), rather

552   than taxonomic composition. Together, our results provide novel insights about the extent and

553   ecological causes of microbiome personalization, and point towards ways to overcome these

554   barriers.

555

556   **Acknowledgments:**

583   Author contributions: EAA, JRB, LBB, RB, JAG, SM, and JT designed the research; EAA,

584   SCA, RB, MRD, LG, JG, LRG, NG, SM, VY, NHL, TLW, RSM, JKW, LS, LBB, and JT,

585   produced the data; JRB, TJG, DAWAMJ, LG, JCG performed the bioinformatics; JRB, KR, SM,

586   performed the statistical analyses. EAA and JRB wrote the manuscript with important

587   contributions from all authors.

24

588   Competing interests: The authors declare no competing interests.

589   Data and materials availability: 16S rRNA gene sequences are deposited on EBI-ENA (project

590   ERP119849) and Qiita [study 12949, (*51*)]. Analyzed data and code is available on the first

591   author's Open Science Framework / GitHub repository; for peer-review purposes, this is an

592   anonymized link: https://osf.io/erdxa/?view_only=3323f05a5a9b479bac1124a5b07a62a9 .

593

594   **References**

595   1.   B. H. Schlomann, R. Parthasarathy, Timescales of gut microbiome dynamics. *Curr Opin*
596   *Microbiol* **50**, 56-63 (2019).
597   2.   H. Koch, P. Schmid-Hempel, Socially transmitted gut microbiota protect bumble bees
598   against an intestinal parasite. *Proceedings of the National Academy of Sciences* **108**,
599   19288-19292 (2011).
600   3.   C. T. Finnicum, J. J. Beck, C. V. Dolan, C. Davis, G. Willemsen, E. A. Ehli, D. I.
601   Boomsma, G. E. Davies, E. J. C. de Geus, Cohabitation is associated with a greater
602   resemblance in gut microbiota which can impact cardiometabolic and inflammatory risk.
603   *BMC Microbiology* **19**, 230 (2019).
604   4.   A. Bashan, T. E. Gibson, J. Friedman, V. J. Carey, S. T. Weiss, E. L. Hohmann, Y. Y.
605   Liu, Universality of human microbial dynamics. *Nature* **534**, 259-262 (2016).
606   5.   E. K. Costello, K. Stagaman, L. Dethlefsen, B. J. Bohannan, D. A. Relman, The
607   application of ecological theory toward an understanding of the human microbiome.
608   *Science* **336**, 1255-1262 (2012).
609   6.   E. T. Miller, R. Svanback, B. J. Bohannan, Microbiomes as metacommunities:
610   understanding host-associated microbes through metacommunity ecology. *Trends in*
611   *Ecology & Evolution*, (2018).
612   7.   J. Bjork, C. Díez-Vives, C. Astudillo-García, E. A. Archie, J. M. Montoya, Vertical
613   transmission of sponge microbiota is inconsistent and unfaithful. *Nature Ecology &*
614   *Evolution* **3**, 1172-1183 (2019).
615   8.   M. Sieber, L. Pita, N. Weiland-Brauer, P. Dirksen, J. Wang, B. Mortzfeld, S.
616   Franzenburg, R. A. Schmitz, J. F. Baines, S. Fraune, U. Hentschel, H. Schulenburg, T. C.
617   G. Bosch, A. Traulsen, Neutrality in the Metaorganism. *PLoS Biol* **17**, e3000298 (2019).
618   9.   A. T. Tredennick, C. dr Mazancourt, M. Loreau, P. B. Adler, Environmental responses,
619   not species interactions, determine synchrony of dominant species in semiarid grasslands.
620   *Ecology* **98**, 971-981 (2017).
621   10.   M. Loreau, C. de Mazancourt, Species synchrony and its drivers: neutral and nonneutral
622   community dynamics in fluctuating environments. *American Naturalist* **172**, E48-66
623   (2008).
624   11.   F. I. Isbell, H. W. Polley, B. J. Wilsey, Biodiversity, productivity and the temporal
625   stability of productivity: patterns and processes. *Ecol Lett* **12**, 443–451 (2009).
626   12.   A. Hector, Y. Hautier, P. Saner, L. Wacker, R. Bagchi, J. Joshi, M. Scherer-Lorenzen, E.
627   M. Spehn, E. Bazeley-White, M. Weilenmann, M. C. Caldeira, P. G. Dimitrakopoulos, J.
628   A. Finn, K. Huss-Danell, A. Jumpponen, C. P. H. Mulder, C. Palmborg, J. S. Pereira, A.
629   S. D. Siamantziouras, A. C. Terry, A. Y. Troumbis, B. Schmid, M. Loreau, General

630   stabilizing effects of plant diversity on grassland productivity through population
631   asynchrony and overyielding. *Ecology* **91**, 2213–2220 (2010).

632   13.   C. de Mazancourt, F. Isbell, A. Larocque, F. Berendse, E. De Luca, J. B. Grace, B.
633   Haegeman, H. W. Polley, C. Roscher, B. Schmid, D. Tilman, J. van Ruijven, A. Weigelt,
634   B. J. Wilsey, M. Loreau, Predicting ecosystem stability from community composition and
635   biodiversity. *Ecology Letters* **16**, 617-625 (2013).

636   14.   K. Gross, B. J. Cardinale, J. W. Fox, A. Gonzalez, M. Loreau, H. W. Polley, P. B. Reich,
637   J. van Ruijven, Species richness and the temporal stability of biomass production: a new
638   analysis of recent biodiversity experiments. *Am Nat* **183**, 1-12 (2014).

639   15.   S. Louca, M. F. Polz, F. Mazel, M. B. N. Albright, J. A. Huber, M. I. O'Connor, M.
640   Ackermann, A. S. Hahn, D. S. Srivastava, S. A. Crowe, M. Doebeli, L. W. Parfrey,
641   Function and functional redundancy in microbial systems. *Nat Ecol Evol* **2**, 936-943
642   (2018).

643   16.   P. B. Rainey, S. D. Quistad, Toward a dynamical understanding of microbial
644   communities. *Philos Trans R Soc Lond B Biol Sci* **375**, 20190248 (2020).

645   17.   G. E. Flores, J. G. Caporaso, J. B. Henley, J. R. Rideout, D. Domogala, J. Chase, J. W.
646   Leff, Y. Vazquez-Baeza, A. Gonzalez, R. Knight, R. R. Dunn, N. Fierer, Temporal
647   variability is a personalized feature of the human microbiome. *Genome Biology* **15**, 531
648   (2014).

649   18.   J. G. Caporaso, C. L. Lauber, E. K. Costello, D. Berg-Lyons, A. Gonzalez, J. Stombaugh,
650   D. Knights, P. Gajer, J. Ravel, N. Fierer, J. I. Gordon, R. Knight, Moving pictures of the
651   human microbiome. *Genome Biology* **12**, R50 (2011).

652   19.   A. J. Johnson, P. Vangay, G. A. Al-Ghalith, B. M. Hillmann, T. L. Ward, R. R. Shields-
653   Cutler, A. D. Kim, A. K. Shmagel, A. N. Syed, S. Personalized Microbiome Class, J.
654   Walter, R. Menon, K. Koecher, D. Knights, Daily Sampling Reveals Personalized Diet-
655   Microbiome Associations in Humans. *Cell Host & Microbe* **25**, 789-802 (2019).

656   20.   D. Rothschild, O. Weissbrod, E. Barkan, A. Kurilshikov, T. Korem, D. Zeevi, P. I.
657   Costea, A. Godneva, I. N. Kalka, N. Bar, S. Shilo, D. Lador, A. V. Vila, N. Zmora, M.
658   Pevsner-Fischer, D. Israeli, N. Kosower, G. Malka, B. C. Wolf, T. Avnit-Sagi, M. Lotan-
659   Pompan, A. Weinberger, Z. Halpern, S. Carmi, J. Fu, C. Wijmenga, A. Zhernakova, E.
660   Elinav, E. Segal, Environment dominates over host genetics in shaping human gut
661   microbiota. *Nature* **555**, 210-215 (2018).

662   21.   G. Falony, M. Joossens, S. Vieira-Silva, J. Wang, Y. Darzi, K. Faust, A. Kurilshikov, M.
663   J. Bonder, M. Valles-Colomer, D. Vandeputte, R. Y. Tito, S. Chaffron, L. Rymenans, C.
664   Verspecht, L. De Sutter, G. Lima-Mendez, K. D'Hoe, K. Jonckheere, D. Homola, R.
665   Garcia, E. F. Tigchelaar, L. Eeckhaudt, J. Fu, L. Henckaerts, A. Zhernakova, C.
666   Wijmenga, J. Raes, Population-level analysis of gut microbiome variation. *Science* **352**,
667   560-564 (2016).

668   22.   A. Zhernakova, A. Kurilshikov, M. J. Bonder, E. F. Tigchelaar, M. Schirmer, T. Vatanen,
669   Z. Mujagic, A. V. Vila, G. Falony, S. Vieira-Silva, J. Wang, F. Imhann, E. Brandsma, S.
670   A. Jankipersadsing, M. Joossens, M. C. Cenit, P. Deelen, M. A. Swertz, R. K. Weersma,
671   E. J. M. Feskens, M. G. Netea, D. Gevers, D. Jonkers, L. Franke, Y. S. Aulchenko, C.
672   Huttenhower, J. Raes, M. H. Hofker, R. J. Xavier, C. Wijmenga, J. Y. Fu, L. C. Study,
673   Population-based metagenomics analysis reveals markers for gut microbiome
674   composition and diversity. *Science* **352**, 565-569 (2016).

675   23.   S. C. Alberts, J. Altmann, "The Amboseli Baboon Research Project: Themes of
676   continuity and change" in *Long-term field studies of primates,* P. Kappeler, D. P. Watts,
677   Eds. (Springer Verlag, 2012), pp. 261-287.
678   24.   L. Grieneisen, M. Dasari, T. J. Gould, J. R. Bjo□rk, J. C. Grenier, V. Yotova, D. Jansen,
679   N. Gottel, J. B. Gordon, N. H. Learn, L. R. Gesquiere, T. L. Wango, R. S. Mututua, J. K.
680   Warutere, I. L. Siod, J. A. Gilbert, L. B. Barreiro, S. C. Alberts, J. Tung, E. A. Archie, R.
681   Blekhman, Gut microbiome heritability is nearly universal but environmentally
682   contingent. *Science* **373**, 181-186 (2021).
683   25.   T. Ren, L. Grieneisen, S. C. Alberts, E. A. Archie, M. Wu, Development, diet, and
684   dynamism: longitudinal and cross-sectional predictors of gut microbial communities in
685   wild baboons. *Environmental Microbiology* **18**, 1312-1325 (2016).
686   26.   L. Grieneisen, M. J. Charpentier, J. Altmann, S. C. Alberts, R. Blekhman, J. Tung, E. A.
687   Archie, Genes, geology, and germs: gut microbiota across a primate hybrid zone are
688   explained by site soil properties, not host species. *Proceedings of the Royal Society* **286**,
689   20190431 (2019).
690   27.   J. B. Silk, Activities and feeding behavior of free-ranging pregnant baboons.
691   *International Journal of Primatology* **8**, 593-613 (1987).
692   28.   S. A. Altmann, *Foraging for Survival: Yearling Baboons in Africa* (University of
693   Chicago Press, Chicago, 1998).
694   29.   A. M. Bronikowski, J. Altmann, Foraging in a variable environment: Weather patterns
695   and the behavioral ecology of baboons. *Behavioral Ecology and Sociobiology* **39**, 11-25
696   (1996).
697   30.   P. Muruthi, J. Altmann, S. Altmann, Resource base, parity and reproductive condition
698   affect females' feeding time and nutrient intake within and between groups of a baboon
699   population. *Oecologia* **87**, 467-472 (1991).
700   31.   J. M. Shopland, Food quality, spatial deployment, and the intensity of feeding
701   interference in yellow baboons (*Papio cynocephalus*). *Behav Ecol Sociobiol* **21**, 149–156
702   (1987).
703   32.   J. Tung, L. B. Barriero, M. B. Burns, J. C. Grenier, J. Lynch, L. E. Grieneisen, J.
704   Altmann, S. C. Alberts, R. Blekhman, E. A. Archie, Social networks predict gut
705   microbiome composition in wild baboons. *eLife* **4**, e05224 (2015).
706   33.   J. T. Morton, C. Marotz, A. Washburne, J. Silverman, L. S. Zaramela, A. Edlund, K.
707   Zengler, R. Knight, Establishing microbial composition measurement standards with
708   reference frames. *Nat Commun* **10**, 2719 (2019).
709   34.   G. B. Gloor, J. M. Macklaim, V. Pawlowsky-Glahn, J. J. Egozcue, Microbiome datasets
710   are compositional: and this is not optional. *Front Microbiol* **8**, 2224 (2017).
711   35.   R. R Core Team, "R: A language and environment for statistical computing. (available at
712   http://www.R-project.org/)" (2020).
713   36.   W. T. Sloan, M. Lunn, S. Woodcock, I. M. Head, S. Nee, T. P. Curtis, Quantifying the
714   roles of immigration and chance in shaping prokaryote community structure.
715   *Environmental Microbiology* **8**, 732-740 (2006).
716   37.   W. T. Sloan, S. Woodcock, M. Lunn, I. M. Head, T. P. Curtis, Modeling Taxa-
717   Abundance Distributions in Microbial Communities using Environmental Sequence Data.
718   *Microbial Ecology* **53**, 443-455 (2007).

Submitted Manuscript: Confidential

719 38. A. R. Burns, W. Zac Stephens, K. Stagaman, S. Wong, J. F. Rawls, K. Guillemin, B. J.
720   Bohannan, Contribution of neutral processes to the assembly of gut microbial
721   communities in the zebrafish over host development. *ISME Journal* **10**, 655-664 (2016).
722 39. D. Sprockett, tyRa: Build Models for Microbiome Data. GitHub repository (available at
723   https://danielsprockett.github.io/tyRa/articles/tyRa.html). (2020).
724 40. J. Oksanen, F. G. Blanchet, M. Friendly, R. Kindt, P. Legendre, D. McGlinn, P. R.
725   Minchin, R. B. O'Hara, G. L. Simpson, P. Solymos, M. Henry, H. Stevens, E. Szoecs, H.
726   Wagner, vegan: Community Ecology Package. R package version 2.5-7. (2020).
727 41. S. N. Wood, Stable and Efficient Multiple Smoothing Parameter Estimation for
728   Generalized Additive Models. *Journal of the American Statistical Association* **99**, 673-
729   686 (2004).
730 42. S. N. Wood, Fast stable restricted maximum likelihood and marginal likelihood
731   estimation of semiparametric generalized linear models. *Journal of the Royal Statistical*
732   *Society: Series B (Statistical Methodology)* **73**, 3–36
733   (2011).
734 43. S. N. Wood, *Generalized Additive Models: An Introduction with R, Second Edition* (CRC
735   Press, 2017).
736 44. A. L. Hicks, K. J. Lee, M. Couto-Rodriguez, J. Patel, R. Sinha, C. Guo, S. H. Olson, A.
737   Seimon, T. A. Seimon, A. U. Ondzie, W. B. Karesh, P. Reed, K. N. Cameron, W. I.
738   Lipkin, B. L. Williams, Gut microbiomes of wild great apes fluctuate seasonally in
739   response to diet. *Nat Commun* **9**, 1786 (2018).
740 45. J. D. Orkin, F. A. Campos, M. S. Myers, S. E. Cheves Hernandez, A. Guadamuz, A. D.
741   Melin, Seasonality of the gut microbiota of free-ranging white-faced capuchins in a
742   tropical dry forest. *ISME J* **13**, 183-196 (2019).
743 46. A. Baniel, K. R. Amato, J. C. Beehner, T. J. Bergman, A. Mercer, R. F. Perlman, L.
744   Petrullo, L. Reitsema, S. Sams, A. Lu, N. Snyder-Mackler, Seasonal shifts in the gut
745   microbiome indicate plastic responses to diet in wild geladas. *Microbiome* **9**, 26 (2021).
746 47. J. P. Mellard, P. Audoye, M. Loreau, Seasonal patterns in species diversity across
747   biomes. *Ecology* **100**, e02627 (2019).
748 48. A. H. Moeller, S. Foerster, M. L. Wilson, A. E. Pusey, B. H. Hahn, H. Ochman, Social
749   behavior shapes the chimpanzee pan-microbiome. *Science Advances* **2**, e1500997 (2016).
750 49. O. Kolodny, M. Weinberg, L. Reshef, L. Harten, A. Hefetz, U. Gophna, M. W. Feldman,
751   Y. Yovel, Coordinated change at the colony level in fruit bat fur microbiomes through
752   time. *Nature Ecology & Evolution* **3**, 116-124 (2019).
753 50. S. Lax, D. P. Smith, J. Hampton-Marcell, S. M. Owens, K. M. Handley, N. M. Scott, S.
754   M. Gibbons, P. Larsen, B. D. Shogan, S. Weiss, J. L. Metcalf, L. K. Ursell, Y. Vazquez-
755   Baeza, W. Van Treuren, N. A. Hasan, M. K. Gibson, R. Colwell, G. Dantas, R. Knight, J.
756   A. Gilbert, Longitudinal analysis of microbial interaction between humans and the indoor
757   environment. *Science* **345**, 1048-1052 (2014).
758 51. A. Gonzalez, J. A. Navas-Molina, T. Kosciolek, D. McDonald, Y. Vazquez-Baeza, G.
759   Ackermann, J. DeReus, S. Janssen, A. D. Swafford, S. B. Orchanian, J. G. Sanders, J.
760   Shorenstein, H. Holste, S. Petrus, A. Robbins-Pianka, C. J. Brislawn, M. Wang, J. R.
761   Rideout, E. Bolyen, M. Dillon, J. G. Caporaso, P. C. Dorrestein, R. Knight, Qiita: rapid,
762   web-enabled microbiome meta-analysis. *Nat Methods* **15**, 796-798 (2018).

763